

Current-voltage correlations in interferometers

Heidi Förster†, Peter Samuelsson‡, M. Büttiker†

† Département de Physique Théorique, Université de Genève, CH-1211 Genève 4, Switzerland

‡ Departement of Solid State Theory, Lund University, Sölvegatan 14 A, S-223 62 Lund, Sweden

Abstract. We investigate correlations of current at contacts and voltage fluctuations at voltage probes coupled to interferometers. The results are compared with correlations of current and occupation number fluctuations at dephasing probes. We use a quantum Langevin approach for the average quantities and their fluctuations. For higher order correlations we develop a stochastic path integral approach and find the generating functions of voltage or occupation number fluctuations. We also derive a generating function for the joint distribution of voltage or occupation number at the probe and current fluctuations at a terminal of a conductor. For energy independent scattering we found earlier that the generating function of current cumulants in interferometers with a one-channel dephasing or voltage probe are identical. Nevertheless, the distribution function for voltage and the distribution function for occupation number fluctuations differ, the latter being wider than that of the former.

PACS numbers: 73.23.-b, 03.65.Yz, 72.70.+m

1. Introduction.

The quantization of charge and the diffraction of quantum waves lead to fluctuations in the transport state of electrical conductors even in the limit of absolute zero temperature [1]. These fluctuations provide additional information not available from conductance measurements alone. This has led to considerable theoretical [2, 3, 4, 5] and experimental efforts [6, 7, 8, 9, 10] to characterize fluctuations not only on the level of noise but including all higher order cumulants. These efforts have been focused almost exclusively on the statistics of transferred charge [2, 3, 4], i.e. on the cumulants of currents measured at a contact of a conductor. Clearly, there are however also other quantities of interest. For example, fluctuations of the charge inside a conductor [11, 12] (as opposed to transferred charge) are closely connected to electrostatic potential fluctuations in a conductor [13] and are thus essential in determining the long range Coulomb interaction of two nearby conductors. Still another example are fluctuations of voltage. The statistics of voltage have been investigated for a mesoscopic conductor in series with a classical impedance [14, 15] and for networks of two-terminal conductors [16].

In this work we consider voltage probes which connect to a conductor within its phase-coherent volume [17]. We determine the fluctuations of the voltage at the probe [18, 19, 20] and determine the joint probability distribution between the voltage fluctuations and the charge transferred into a contact of the conductor. Voltage probes are real elements of mesoscopic conductors and are used to gain information of the interior state of the system. We compare the fluctuations at a voltage probe with the fluctuations at a dephasing probe. This latter probe conserves not only charge but also energy [21]. At a dephasing probe the occupation number fluctuates [19]. Voltage and dephasing probes provide a simple means to introduce incoherent events in an otherwise quantum coherent conductor [17, 21].

We examine these correlations with the help of a (quantum) Langevin approach [22, 23]. In a second step we derive a generating function for the correlations using a semi-classical path integral approach [24, 25]. On the level of conductance and noise the Langevin approach and the saddle point solution of the path integral approach are shown to agree. We have earlier demonstrated that for the statistics of transferred charge both a single channel voltage probe and the single channel dephasing probe lead to the same counting functional if the scattering matrix of the conductor is energy independent in the range of applied voltages [24, 25]. Interestingly, we find that this equivalence does not hold for the joint distribution of voltage (or occupation number) fluctuations and transferred charge.

The characterization of the transport fluctuations not only in terms of transferred charges but also of internal properties is a central motivation of this work. Voltage fluctuations at a probe test carrier fluctuations that can still be evaluated in an approach that considers samples with terminals only. It is particularly interesting for conductors which exhibit quantum interference since voltage and dephasing probes are phase breaking elements. A carrier that enters a probe is eventually replaced by a carrier that is re-emitted into the conductor with a phase (and in the case of a voltage probe, an energy) that is unrelated to the exiting carrier. This carrier is detected in the voltage probe and thus does not contribute to certain interference processes. The correlation of the voltage and the transferred charge stems from incoherent processes. Indeed, phase breaking and which path detection are generally closely linked phenomena [26]. This provides another motivation to investigate the

fluctuations at the probes (the which path detectors) and their correlations with the transmitted current.

2. Correlations: Langevin approach.

The Langevin approach is a convenient tool to investigate current and voltage correlations in mesoscopic conductors [22, 23]. This has been demonstrated in numerous papers, see e.g. Refs. [1, 18, 19, 27, 28, 29, 30]. Importantly, the Langevin approach also allows one to obtain information on the fluctuation properties of a probe connected to the mesoscopic conductor. In this section we investigate the average current and potentials as well as the auto- and cross-correlations. It is possible to extend the Langevin approach successively to higher order correlations, giving rise to cascade corrections [5]. In section 3 we instead directly determine the generating function of the correlations, making use of a stochastic path integral approach [4].

We consider a multi terminal quantum coherent conductor first without being connected to a probe. The current through the conductor fluctuates. When the conductor is embedded in a zero-impedance external circuit, all contacts are characterized by Fermi distribution functions which are constant in time. Only bare current fluctuations take place due to scattering in the conductor, described by a unitary scattering matrix \mathcal{S} . The total current in contact α can be expressed as a sum of the average current and the current fluctuations [22, 23]

$$I_\alpha = \langle I_\alpha \rangle + \delta I_\alpha = \sum_\beta G_{\alpha\beta} V_\beta + \delta I_\alpha, \quad (1)$$

where V_β is a voltage applied to reservoir β , and $G_{\alpha\beta}$ the conductance matrix

$$G_{\alpha\beta} = \frac{e^2}{h} \int dE \left(-\frac{\partial f}{\partial E} \right) [N_\alpha \delta_{\alpha\beta} - T_{\alpha\beta}]. \quad (2)$$

The equilibrium Fermi function is called f , the number of channels in lead α is N_α , and $T_{\alpha\beta} = T_{\alpha\beta}(E) = \text{Tr}[\mathcal{S}_{\alpha\beta}^\dagger(E) \mathcal{S}_{\alpha\beta}(E)]$ denotes the total probability that a particle is transmitted from terminal β to terminal α where the trace runs over the transport channels.

Like the conductances, the noise correlations can be expressed in terms of scattering matrices. The zero frequency noise and correlations are $C_{\alpha\beta} = \langle \delta I_\alpha \delta I_\beta \rangle$. Note that the definition of the noise as given for example in Ref. [1] usually differs by a factor of 2. The noise can be expressed as $C_{\alpha\beta} = C_{\alpha\beta}^{eq} + C_{\alpha\beta}^{tr}$, a sum of an equilibrium contribution $C_{\alpha\beta}^{eq}$ stemming from noisy incident beams in one contact proportional to $f_\alpha(1 - f_\alpha)$, and a transport contribution $C_{\alpha\beta}^{tr}$ which depends on Fermi functions of two different reservoirs $f_\gamma(1 - f_\delta)$ (with $\gamma \neq \delta$). Following Ref. [23] we find

$$C_{\alpha\beta}^{eq} = \frac{e^2}{h} \int dE (2\delta_{\alpha\beta} N_\alpha f_\alpha (1 - f_\alpha) - \text{Tr}[T_{\beta\alpha}] f_\alpha (1 - f_\alpha) - \text{Tr}[T_{\alpha\beta}] f_\beta (1 - f_\beta)), \quad (3)$$

$$C_{\alpha\beta}^{tr} = \frac{e^2}{2h} \int dE \sum_{\gamma, \delta} \text{Tr}[\mathcal{S}_{\alpha\gamma}^\dagger \mathcal{S}_{\alpha\delta} \mathcal{S}_{\beta\delta}^\dagger \mathcal{S}_{\beta\gamma}] (f_\gamma (1 - f_\delta) + f_\delta (1 - f_\gamma) - 2f_\alpha (1 - f_\alpha)). \quad (4)$$

In the case when temperature is negligible compared to the applied bias, the contribution $C_{\alpha\beta}^{eq}$ vanishes and the term $C_{\alpha\beta}^{tr}$ represents the pure shot noise.

2.1. Voltage probe.

A voltage probe is a large metallic contact connected to the conductor. The potential V_p at the contact is left floating and there is no current drawn at the probe. The potential $V_p = V_p(t)$ exhibits fluctuations on the time scale τ_d , which is given by the RC -time of a classical circuit. The fluctuations originate from the response of the potential to the injected charges: Incoming charges make the potential V_p rise. This leads in turn to an increase in the outgoing current which reduces the potential again and so on. This mechanism is formally expressed by vanishing current and current fluctuations at the probe for frequencies smaller than $1/\tau_d$:

$$\langle I_p \rangle = 0, \quad \Delta I_p = 0. \quad (5)$$

The voltage probe is described by an equilibrium Fermi function $f_p(V_p)$, where thermalization by inelastic scattering is assumed to be much faster than the delay time τ_d , and where the temperature is determined by the lattice temperature. Therefore, a particle scattering via the voltage probe loses not only its phase memory but also changes its energy.

The potential fluctuations at the probe give rise to additional fluctuations of the current in the terminals [18, 19]. The potential at the probe can be separated into a constant and a fluctuating part, $V_p = \bar{V}_p + \Delta V_p$. Following Eq. (1) the average current $\langle I_\alpha \rangle$ and the total fluctuations ΔI_α are in linear response given by

$$\langle I_\alpha \rangle = \sum_{\beta \neq p} G_{\alpha\beta} V_\beta + G_{\alpha p} \bar{V}_p, \quad (6)$$

$$\Delta I_\alpha = G_{\alpha p} \Delta V_p + \delta I_\alpha. \quad (7)$$

Both the constant value \bar{V}_p and the fluctuating part ΔV_p of the potential at the probe are determined by the condition Eq. (5). Throughout this paper we consider that only one of the contacts (taken to be $\alpha = 1$) has an elevated potential eV and all other current terminals are grounded. Solving Eqs. (6) and (7) with $\alpha = p$, the potential at the probe is found to be $\bar{V}_p = -G_{p1}V/G_{pp}$, and $\Delta V_p = -\delta I_p/G_{pp}$. Using this we find for the auto-correlations of the potential and the cross correlations of the potential with the current in terminal α

$$\langle \Delta V_p^2 \rangle = \langle \delta I_p^2 \rangle / G_{pp}^2 = \frac{C_{pp}}{G_{pp}^2}, \quad (8)$$

$$\langle \Delta V_p \Delta I_\alpha \rangle = \left(\frac{G_{\alpha p}}{G_{pp}} \langle \delta I_p^2 \rangle - \langle \delta I_p \delta I_\alpha \rangle \right) / G_{pp} = \frac{G_{\alpha p} C_{pp}}{G_{pp}^2} - \frac{C_{p\alpha}}{G_{pp}}. \quad (9)$$

These expressions can be evaluated for a given scattering matrix using Eqs. (2), (3) and (4), where only the constant Fermi functions enter, i.e. $f_p = f_p(\bar{V}_p)$. For higher order correlations the fluctuations of the Fermi functions have to be taken into account. As pointed out above, this leads to noise of noise and results in a cascade corrections similar to the one known from the quasi-classical fluctuating Boltzmann equation [5].

2.2. Dephasing probe.

Dephasing probes are a conceptual tool to describe quasi-elastic dephasing [21]. In the case of a dephasing probe, a particle entering the probe is incoherently re-emitted within the same energy interval $[E, E + dE]$. It loses its phase, but the change in energy dE is much smaller than the external bias or the temperature. Because scattering in each energy interval is independent, the distribution function $n_p(E)$ is

-unlike the Fermi function describing the voltage probe- a highly non-equilibrium distribution function. It shows independent fluctuations in each energy interval, $n_p(E) = n_p(E, t)$, which occur on the time scale τ_d , the delay time of the probe. In a dephasing probe, the current per energy interval $i_p(E)$ and its fluctuations are conserved up to the frequency $1/\tau_d$:

$$\langle i_p \rangle = 0, \quad \Delta i_p = 0. \quad (10)$$

Similar to the potential of the voltage probe, the non-equilibrium distribution function is written as a constant and a fluctuating part $f_p \equiv \bar{n}_p + \Delta n_p$. All other terminals are still characterized by constant equilibrium Fermi functions. The average current per energy $\langle i_\alpha(E) \rangle = \langle i_\alpha \rangle$ and the total current fluctuations per energy $\Delta i_\alpha(E) = \Delta i_\alpha$ are given by

$$\langle i_\alpha \rangle = \sum_{\beta \neq p} g_{\alpha\beta} f_\beta + g_{\alpha p} \bar{n}_p, \quad (11)$$

$$\Delta i_\alpha = g_{\alpha p} \Delta n_p + \delta i_\alpha. \quad (12)$$

In analogy to the expressions for the energy integrated current $I_\alpha = \int dE i_\alpha(E)$, an energy dependent conductance matrix $g_{\alpha\beta} = g_{\alpha\beta}(E)$ can be defined,

$$g_{\alpha\beta} = \frac{e}{h} [N_\alpha \delta_{\alpha\beta} - T_{\alpha\beta}]. \quad (13)$$

Also for the zero-frequency noise we find an energy dependent function from $C_{\alpha\beta} = \int dE c_{\alpha\beta}(E)$. Again the function $c_{\alpha\beta} = c_{\alpha\beta}(E) = \langle \delta i_\alpha \delta i_\beta \rangle$ splits into an equilibrium and a transport contribution

$$c_{\alpha\beta} = c_{\alpha\beta}^{eq} + c_{\alpha\beta}^{tr}, \quad (14)$$

where $c_{\alpha\beta}^{eq}$ and $c_{\alpha\beta}^{tr}$ are the integrands of Eqs. (3) and (4) respectively. $c_{\alpha\beta}^{eq}$ contains the noise due to a noisy incident beam in one contact, while $c_{\alpha\beta}^{tr}$ involves particles from two different contacts.

Using Eq. (10) the noise and correlations at the probe are [19, 31]

$$\langle \Delta n_p^2 \rangle = \langle \delta i_p^2 \rangle / g_{pp}^2 = \frac{c_{pp}}{g_{pp}^2}, \quad (15)$$

$$\langle \Delta n_p \Delta i_\alpha \rangle = \left(\frac{g_{\alpha p}}{g_{pp}} \langle \delta i_p^2 \rangle - \langle \delta i_p \delta i_\alpha \rangle \right) / g_{pp} = \frac{g_{\alpha p} c_{pp}}{g_{pp}^2} - \frac{c_{p\alpha}}{g_{pp}}. \quad (16)$$

Here we can see the first consequence of the different electron distributions (see Fig. 1) in the voltage and dephasing probe. Although Eqs. (8), (9) and (15), (16) have exactly

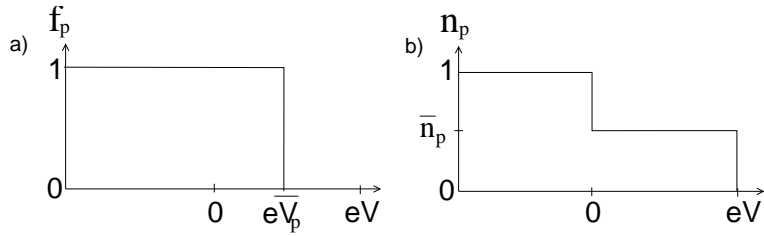


Figure 1. a) The Fermi distribution function of the voltage probe takes on only the values zero or one (at zero temperature). The position of the step is given by the potential at the probe. b) The distribution function of the dephasing probe is a two-step function and has a value between zero and one in the interval $[0, eV]$.

the same structure, the evaluation leads to different results. The reason is that in the case of a voltage probe the contribution $C_{\alpha\beta}^{eq}$ to the noise vanishes at zero temperature, while for a dephasing probe, the corresponding expression $c_{\alpha\beta}^{eq}$ is non-zero even at zero temperature since the factor $\bar{n}_p(1-\bar{n}_p)$ is finite in the energy interval $[0, eV]$ of interest.

2.3. Correlations and interference.

It is interesting to investigate how and if interference appears in the fluctuations of the potential and the occupation number of the probe or in the correlations with the current in one of the leads. To this end we evaluated Eqs. (8), (9) and (15), (16) for four different setups: a beam splitter and three interfering systems, the Mach-Zehnder interferometer, the double barrier and the triple barrier.

These examples also illustrate an interesting feature of the different nature of voltage and dephasing probes. It was shown in Refs. [24, 25] that the auto- and cross correlations (actually all cumulants) of the current in a conductor coupled to a single mode probe are independent of whether the probe is a voltage or a dephasing probe for the case that scattering is energy independent. Interestingly, this does not hold for the fluctuations of the probe: there is a clear difference between the potential fluctuations of a voltage probe and the occupation number fluctuations of the dephasing probe.

All the examples are quantum Hall bars of different complexity subject to a high magnetic field. Current is transported by an edge state at filling factor one, where carriers move in one specific direction along the edge of the structure. A quantum point contact in such a structure forms a beam splitter: a particle is either transmitted and continues along the same edge, or it is reflected and moves into the opposite direction along the opposite edge. The beam splitter is the smallest unit that the interfering structures are composed of, we chose it here as a simple and instructive example to show how a voltage or dephasing probe behaves. For simplicity we consider the scattering matrix of all structures to be energy independent. In the following we present briefly the setups of the four examples. The results are collected in table 1 and table 2.

- The **beam splitter** [32, 33] is formed by a quantum point contact with

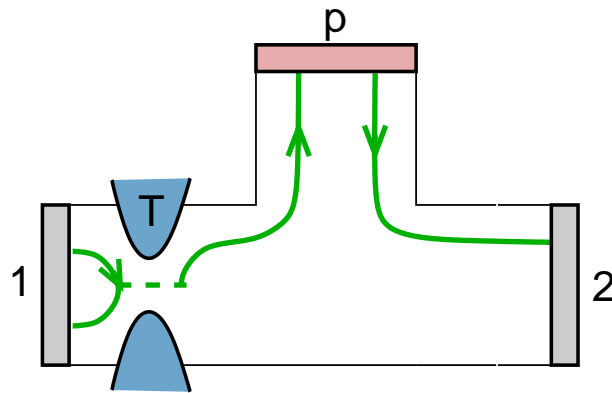


Figure 2. A quantum point contact in the quantum Hall regime forms a beam splitter with transmission probability T . A perfectly coupled probe is attached along the upper edge.

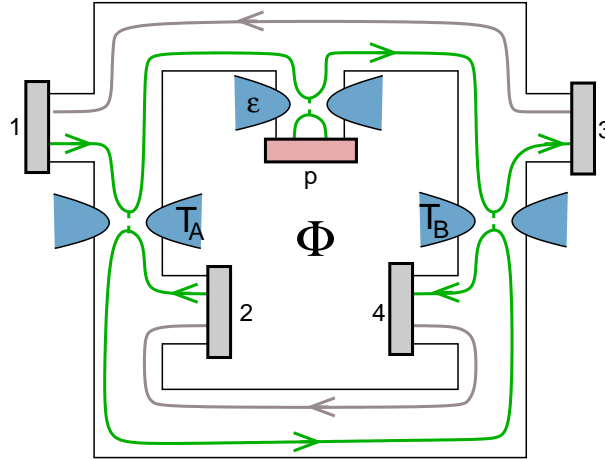


Figure 3. A Mach-Zehnder interferometer with its upper arm coupled to a dephasing or voltage probe with coupling strength ε . An Aharonov-Bohm flux generates a phase Φ .

transmission probability T , situated between two terminals 1 and 2, as shown in Fig. 2. A probe -either a voltage or a dephasing probe- is perfectly coupled to the setup, such that every particle transmitted through the beam splitter enters the probe and moves then from the probe into contact 2.

- An electronic **Mach-Zehnder interferometer** (MZI) is shown in Fig. 3. It consists of two arms connected to four electronic reservoirs 1 to 4 via beam splitters A and B . The transmission (reflection) probabilities of the beam splitters are T_A and T_B (R_A and R_B) respectively. Interference occurs, because the electrons have two alternative paths to propagate through the interferometer between beam splitter A and B . An Aharonov-Bohm flux threads the two arms, and the different vector potentials in the two arms lead to a phase difference Φ . This difference creates a characteristic flux-periodicity in the interference pattern, the Aharonov-Bohm effect. Thus the Mach-Zehnder interferometer is useful as a conceptually simple interferometer and has been used in theoretical discussions of dephasing [34, 35, 36, 37, 38]. Such a setup was recently realized experimentally [39, 40, 41] and has since generated further works [42, 43, 44]. If the length of the two interferometer arms is not equal, the transmission through the interferometer will be energy dependent due to the geometric phase a particle acquires. For finite temperature, interference effects will be averaged out. In order to determine purely the effect of dephasing and voltage probes, we concentrate here on the ideal case of an equal arm lengths interferometer.
- The **double barrier**, shown in Fig. 4, is a two terminal conductor with two beam splitters [45, 46]. In the region between the barriers (the dot) a particle can perform multiple loops and undergo resonant scattering. For each loop in the dot, the electron picks up a phase Φ_d . We consider zero temperature and an energy independent phase. The interference is here not a consequence of two spatially distinct paths but of multiple possible paths through the closed orbit inside the dot. A probe is coupled to the dot with coupling strength ε . Since particles that scatter via the probe loose their phase, coherence is partially destroyed. For

perfect coupling, $\varepsilon = 1$, all particles entering the dot pass on into the probe, then the system is incoherent and in the sequential tunneling regime.

- In the **triple barrier** setup, an additional barrier in series is inserted into the double barrier setup, see Fig. 5. Now there are two dots [47, 48, 49] with two different phases Φ_L and Φ_R . Resonances can occur in either one of the dots or through both dots simultaneously, rendering the scattering matrix considerably more complex. The limiting case $R_2 \rightarrow 0$ however represents the double barrier with $\Phi_L + \Phi_R = \Phi_d$. We consider here a probe coupled to the left dot, thus only the interference in the left dot is destroyed by the probe.

In table 1 the results for the auto-correlations of the voltage $\langle \Delta V_p^2 \rangle$ and of the occupation number $\langle \Delta n_p^2 \rangle$ are listed. The different electron distributions of voltage and dephasing probes, as pointed out already in section 2.2, become apparent: the fluctuations of the occupation number $\bar{n}_p(E)$ in a dephasing probe are larger than the potential fluctuations of the voltage probe. This is most easily seen in the example of the beam splitter, where the fluctuations of $\bar{n}_p(E)$ are twice as large as the fluctuations of \bar{V}_p . Note that occupation numbers at different energies are uncorrelated but that the fluctuation spectrum, in the limit of zero temperature, and in the limit that the energy dependence of the scattering matrix can be neglected, is independent of energy for $0 \leq E \leq eV$.

For finite coupling, the fluctuations are proportional to $1/\varepsilon$ and diverge for $\varepsilon \rightarrow 0$ for both voltage and dephasing probe. This means the fewer particles enter the probe,

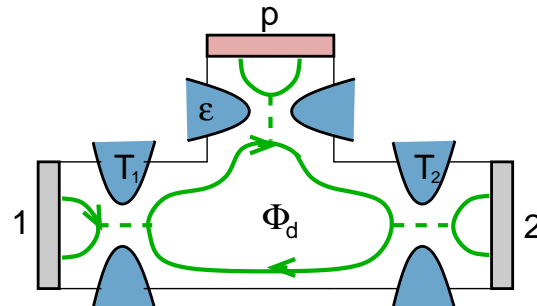


Figure 4. The double barrier quantum Hall interferometer with a resonant state. A probe couples to the resonant state with coupling strength ε . Φ_d is the total phase acquired in one loop.

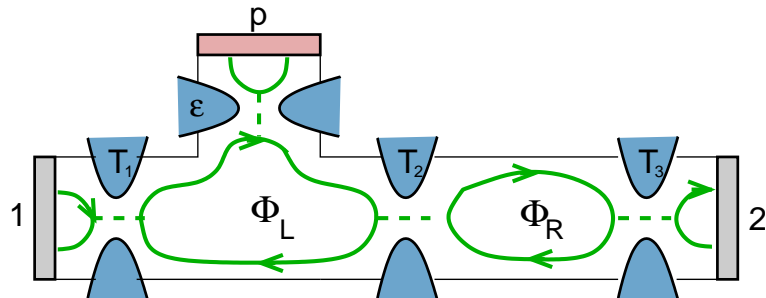


Figure 5. The triple barrier with two resonant states. A single probe is coupled to the left resonant state.

Table 1. The mean squared fluctuations of the potential and the occupation number for the four examples. The transmission probabilities of all point contacts in the double and triple barrier structures are equal, $T = 1 - R$. Interference effects are present only in the latter two.

	$\langle \Delta V_p^2 \rangle \frac{e}{hV}$	$\langle \Delta n_p^2 \rangle \frac{1}{h}$
Beam splitter	$T(1 - T)$	$2T(1 - T)$
Mach-Zehnder interferometer	$\frac{2-\varepsilon}{\varepsilon} T_A(1 - T_A)$	$\frac{2}{\varepsilon} T_A(1 - T_A)$
Double barrier	$\frac{R((1+R^2)(2-\varepsilon)+4R\sqrt{1-\varepsilon}\cos\Phi_d)}{\varepsilon(1-R)(1+R)^3}$	$\frac{2R(1+R^2(1-\varepsilon)+2R\sqrt{1-\varepsilon}\cos\Phi_d)}{\varepsilon(1-R)(1+R)^3}$
Triple barrier	$\frac{R}{\varepsilon} \mathcal{F}(R, \Phi_R) [(1+3R^2)(2-\varepsilon) + 4R(1+R)\sqrt{1-\varepsilon}\cos\Phi_L + 4R^2\sqrt{1-\varepsilon}\cos(\Phi_L - \Phi_R) + 2R(1+R)(2-\varepsilon)\cos\Phi_R + 4R\sqrt{1-\varepsilon}\cos(\Phi_L + \Phi_R)]$ <p>with</p> $\mathcal{F}(R, \Phi_R) = \frac{1+R^2+2R\cos\Phi_R}{(1+R+2R\cos\Phi_R)^3}$	$\frac{2R}{\varepsilon} \mathcal{F}(R, \Phi_R) [1+3R^2-2R^2\varepsilon + 2R(1+R)\sqrt{1-\varepsilon}\cos\Phi_L + 2R^2\sqrt{1-\varepsilon}\cos(\Phi_L - \Phi_R) + 2R(1+R(1-\varepsilon))\cos\Phi_R + 2R\sqrt{1-\varepsilon}\cos(\Phi_L + \Phi_R)]$

the stronger are the fluctuations. Note that the fluctuations of voltage and dephasing probe coincide to first order in the coupling parameter ε , only processes of second order in ε contribute to the differences. (For the beam splitter, the table includes only the strong coupling result $\varepsilon = 1$. The above statement applies also to the beam splitter with a weakly coupled probe).

The noise of the probe in the MZI is independent of the phase Φ . This is not surprising since particles enter the probe before they could interfere. This is in accordance with Ref. [34] which demonstrates that charge density fluctuations in an MZI arm are independent of phase. In the double barrier, particles enter the probe after performing multiple loops inside the dot and thus the fluctuations depend on the phase Φ_d picked up. In the triple barrier different paths containing different resonant passages are possible and the noise contains a combination of Φ_L , Φ_R , $\Phi_L + \Phi_R$ and $\Phi_L - \Phi_R$.

Table 2 shows the correlations of the voltage fluctuation measured at a probe with the current transferred into a contact. As usual p denotes the probe and α stands for any of the contacts of the conductor. At first we note that the energy integrated correlations $\langle \Delta V_p \Delta I_\alpha \rangle / V$ equal the correlations $\langle \Delta n_p \Delta i_\alpha \rangle$ which characterize an energy interval in the window opened by the transport voltage eV . This equivalence

Table 2. Current voltage correlations $\langle \Delta V_p \Delta I_\alpha \rangle$ and current occupation number fluctuations $\langle \Delta n_p \Delta i_\alpha \rangle$. For energy independent scattering these two correlations are identical.

	$\langle \Delta V_p \Delta I_\alpha \rangle \frac{1}{eV} = \langle \Delta n_p \Delta i_\alpha \rangle \frac{1}{e}$
Beam splitter	$\pm T(1 - T)$ for $\alpha = 1$ (+) and $\alpha = 2$ (-)
Mach-Zehnder interferometer	$T_A(1 - T_A)(1 - 2T_B)$ for $\alpha = 3$
Double barrier	$-\frac{R(1-R)}{(1+R)^3}$ for $\alpha = 2$
Triple barrier	$R(1 - R)\mathcal{F}(R, \Phi_R)[-1 + 3R + 2R \cos \Phi_R]$ for $\alpha = 2$

is again a consequence of the energy independent scattering assumed here.

The example of the beam splitter shows that the correlation can have either sign, depending on whether we consider the correlation with the transmitted ($\alpha = 2$) or the reflected ($\alpha = 1$) particle current. The dependence on the transmission probability directly reflects the shot noise generated at the quantum point contact.

The correlations in the MZI are independent of the phase Φ . The correlations are a signature of incoherent processes: only carriers that enter the probe give rise to voltage fluctuations and only carriers that leave from the probe to the contact are correlated with the voltage at the probe. Note, that the additional beam splitter B the particles have to pass after leaving the probe renders the correlations cubic in the transmission of the beam splitters (in contrast to the beam splitter setup of the first example). Curiously, for $T_A = T_B = T$ they coincide with the third current cumulants [2, 37] of a beam splitter with transmission T . In contrast to the simple beam splitter (first example) here the correlation changes sign as function of the transmission probability of the second beam splitter T_B . For $T_B = 1$ we have the same situation as for the beam splitter with $\alpha = 2$, and $T_B = 0$ corresponds to the beam splitter result for $\alpha = 1$.

Surprisingly, also the correlations for the double barrier are independent of the phase Φ_d . Technically the reason is that the correlations Eqs. (9) and (16) are of the form "current correlations over conductance", and the oscillating contributions in the involved functions drop out. The noise in Eqs. (8) and (15) is of the form "fluctuations over (conductance)²", and the interference is present. For the case when the two barriers have unequal transmission probabilities, the beam splitter example can be recovered by setting $T_2 = 1$.

In the triple barrier a probe is only connected to the left dot. The correlations of the triple barrier contain the phase Φ_R due to interference in the right dot but are independent of Φ_L . This is consistent with the fact that the correlation for the double barrier is independent of phase.

All correlations shown in table 2 are independent of the coupling strength of the probe and moreover are independent of the phase directly adjacent to the probe. Further research is needed to demonstrate whether these features are generic or special for the examples investigated here.

3. Full counting statistics of the probe: the stochastic path integral.

An elegant description of the zero frequency transport is the full counting statistics (FCS) [2, 3, 5] which permits to obtain not only the average current and noise but the full distribution of charges transmitted through a conductor during a measurement time τ . For an M -terminal conductor without a probe the distribution function is denoted by $P(\mathbf{Q})$, where the vector quantity $\mathbf{Q} = (Q_1, Q_2, \dots, Q_M)$ describes the charge transferred into each of the M terminals. $P(\mathbf{Q})$ can be expressed in terms of the cumulant generating function $S(\mathbf{\Lambda})$, where $\mathbf{\Lambda} = (\lambda_1, \lambda_2, \dots, \lambda_M)$ are the conjugate variables to \mathbf{Q} :

$$P(\mathbf{Q}) = \int d\mathbf{\Lambda} e^{S(\mathbf{\Lambda}) - i\mathbf{\Lambda} \cdot \mathbf{Q}}, \quad (17)$$

$$S(\mathbf{\Lambda}) = \ln \sum_{\mathbf{Q}} P(\mathbf{Q}) e^{i\mathbf{\Lambda} \cdot \mathbf{Q}}. \quad (18)$$

The sum and integrals run over all elements of the vector, $\int d\mathbf{\Lambda} = (2\pi)^{-M} \int d\lambda_1 \dots d\lambda_M$ and $\sum_{\mathbf{Q}} = \sum_{Q_1, \dots, Q_M}$. Probability conservation leads to the normalization of the generating function $S(\mathbf{0}) = 0$.

For a long measurement time τ , the transmitted charge into a contact α is proportional to τ : $Q_\alpha = \tau I_\alpha$. Then the zero frequency current cumulants are obtained by taking derivatives of the cumulant generating function with respect to the counting variables and evaluated at $\mathbf{\Lambda} = 0$. The average current $\langle I_\alpha \rangle$ and the auto- and cross-correlations $C_{\alpha\beta}$ are given by

$$\langle I_\alpha \rangle = \frac{e}{i\tau} \frac{dS}{d\lambda_\alpha}, \quad C_{\alpha\beta} = \frac{e^2}{i^2 \tau} \frac{d^2 S}{d\lambda_\alpha d\lambda_\beta}. \quad (19)$$

When a probe is connected to the conductor, particles can enter and leave the probe. However, for every particle entering the probe, a particle is re-emitted after a delay time τ_d as described in sections 2.1 and 2.2. The functions $P(\mathbf{Q})$ and $S(\mathbf{\Lambda})$ have then to be determined under the condition that no charge is accumulated in the probe. The transport statistics under this constraint was developed in Refs. [24, 25] using a stochastic path integral approach. The findings are that the model of voltage and dephasing probes are perfectly equivalent for the case of one single-channel probe. For multi-channel or multiple probes the transport statistics of voltage and dephasing probes differs.

Here we address the question of whether information about the statistics of the probe itself can be obtained. Usually the quantities investigated with the FCS are the number of charges $\mathbf{Q} = \int_0^\tau dt \mathbf{I}(t)$ counted during a measurement time τ . Consequently, we now need to consider the statistics of the quantities $\int dt V_p(t)$ and $\int dt n_p(t)$. More precisely we are interested in for example $\frac{1}{\tau} \int dt dt' \langle V_p(t) V_p(t') \rangle$

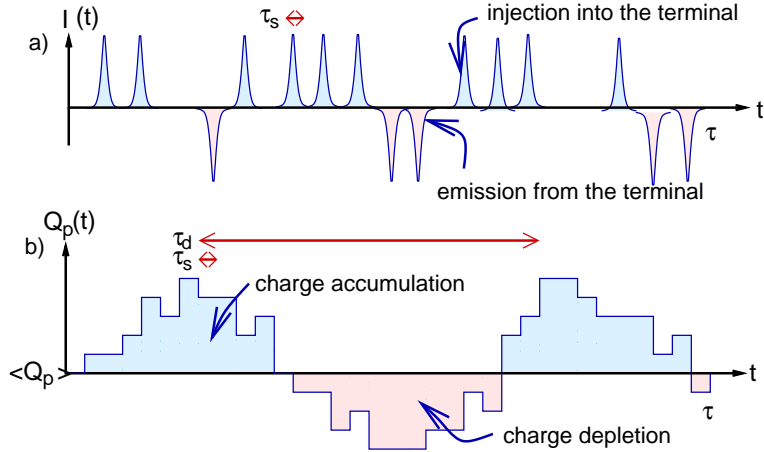


Figure 6. a) The current as a function of time at a terminal. The charge transferred into a terminal is absorbed immediately. For a one-channel contact only one charge per time step $\tau_s = h/eV$ can enter. b) Charge on a voltage (dephasing) probe as a function of time. The charge on the probe accumulates and fluctuates on the time scale τ_d , the delay time of the probe. The figure is for $\tau_d \gg \tau_s$.

or $\frac{1}{\tau} \int dt dt' \langle n_p(t) n_p(t') \rangle$. For the voltage probe we can define a normalized phase ϕ_p proportional to the time integrated voltage and for the dephasing probe a time averaged occupation number $\bar{n}_p = \bar{n}_p(E)$,

$$\phi_p = \frac{1}{N} \frac{e}{h} \int_0^\tau dt V_p(t) = \frac{1}{V\tau} \int_0^\tau dt V_p(t), \quad (20)$$

$$\bar{n}_p = \frac{1}{\tau} \int_0^\tau dt n_p(E, t), \quad (21)$$

where $N = eV\tau/h$. These are the accessible quantities describing the probe, they are not numbers of particles but phases. This is a consequence of the fact that charges transferred into the terminals are absorbed, but the charge on the probe is conserved. Fig. 6 illustrates this difference. Both ϕ_p and \bar{n}_p vary from measurement to measurement, because the injection of particles into the probe that determines the time averaged potential and the time averaged occupation number is a probabilistic process. The phase ϕ_p is proportional to the total charge on the probe integrated during the measurement time τ : $\phi_p = \frac{e}{CNh} \int_0^\tau dt Q_p(t)$, with C the capacitance of the voltage probe. In Refs. [11] and [12] the FCS of charge fluctuations in a chaotic cavity were investigated, conceptually this is similar to the FCS of ϕ_p addressed here. As pointed out in Ref. [11], the quantity $\int_0^\tau dt Q_p(t)$ has no direct physical meaning, but can be understood as the time spent by all electrons in the cavity (or probe) after time τ , or alternatively as the phase picked up due to the potential integrated over time τ . In analogy to this, the phase \bar{n}_p is proportional to the charge in an energy interval dE integrated during τ . We only consider the case that there is a large number of states in this energy interval. This corresponds to the case of a long delay time τ_d of particles inside the probe. For the stochastic path integral approach discussed here it is important that the charge on the probe is slowly fluctuating compared to the inverse attempt frequency $\tau_s = h/eV$: $\tau_d \gg \tau_s$. This allows to justify the saddle

point solutions which will be used later on. A different dynamics at voltage probes is considered in Ref. [51].

3.1. Voltage probe.

We define a joint probability $P(\mathbf{Q}, \phi_p)$ that \mathbf{Q} charges are transmitted during τ and the phase due to the potential of the voltage probe is ϕ_p . By definition we have $P(\mathbf{Q}) = \int_0^1 d\phi_p P(\mathbf{Q}, \phi_p)$. The conjugated variable to ϕ_p is a number called m_p . Fourier transforms in the variables \mathbf{Q} or ϕ_p or in both of them are possible. Thus there are four equivalent functions containing all informations about the transport and the probe statistics: $P(\mathbf{Q}, \phi_p)$, $S(\mathbf{\Lambda}, m_p)$, $\xi(\mathbf{\Lambda}, \phi_p)$ and $\zeta(\mathbf{Q}, m_p)$. Note that the counting fields $\mathbf{\Lambda}$ are periodic in 2π , but ϕ_p has a period of 1. Thus the exponent in the transformation is multiplied by 2π . Explicitly written we have for example,

$$P(\mathbf{Q}, \phi_p) = \int d\mathbf{\Lambda} \sum_{m_p} e^{S(\mathbf{\Lambda}, m_p) - i\mathbf{\Lambda}\mathbf{Q} - 2\pi i\phi_p m_p}, \quad (22)$$

$$P(\mathbf{Q}, \phi_p) = \int d\mathbf{\Lambda} e^{\xi(\mathbf{\Lambda}, \phi_p) - i\mathbf{\Lambda}\mathbf{Q}}. \quad (23)$$

In particular we are interested in the distribution $P(\phi_p)$ of the phase ϕ_p alone. It is obtained from the relation

$$P(\phi_p) = \sum_{\mathbf{Q}} P(\mathbf{Q}, \phi_p) = e^{\xi(\mathbf{\Lambda}=\mathbf{0}, \phi_p)}. \quad (24)$$

Refs. [24, 25] used the stochastic path integral to calculate the generating function of a conductor coupled to a voltage or dephasing probe. With this formalism also the joint functions P, S, ξ and ζ introduced above are accessible. A description of the procedure is given in the appendix, here we simply state the results.

Most directly the function $\xi(\mathbf{\Lambda}, \phi_p)$ can be determined by an integral

$$e^{\xi(\mathbf{\Lambda}, \phi_p)} = \int d\lambda_p e^{\bar{S}_V(\mathbf{\Lambda}, \lambda_p, V_p=V\phi_p)}. \quad (25)$$

A very long measurement time $\tau \gg \tau_d$ defines the stationary case considered here where the variables λ_p and V_p are time independent. The function $\bar{S}_V(\mathbf{\Lambda}, \lambda_p, V_p)$ is given by [50]

$$\bar{S}_V(\mathbf{\Lambda}, \lambda_p, V_p) = \frac{\tau}{h} \int dE H_0 \quad (26)$$

with

$$H_0 = \ln \det \left[1 + \tilde{n} \left(\tilde{\lambda}^\dagger \mathcal{S}^\dagger \tilde{\lambda} \mathcal{S} - 1 \right) \right]. \quad (27)$$

For a conductor with single mode contacts to the M terminals and to the probe, the scattering matrix \mathcal{S} is of dimension $(M+1) \times (M+1)$. The matrix \tilde{n} contains the occupation numbers of the different terminals with $\tilde{n} = \text{diag}(n_1, n_2, \dots, n_M, n_p)$ (here $n_p \equiv f_p(V_p)$), and the matrix $\tilde{\lambda}$ introduces the counting fields, $\tilde{\lambda} = \text{diag}(e^{i\lambda_1}, e^{i\lambda_2}, \dots, e^{i\lambda_M}, e^{i\lambda_p})$.

To proceed it is useful to introduce the expressions q_{kl} containing multi-particle scattering probabilities multiplied with the appropriate counting fields in the contacts. The index $l = 0, 1$ denotes the number of particles injected into the probe, and $k = 0, 1$ the number of particles emitted from the probe [25]. Below, for the examples of interest

here, we give the explicit expressions for the q_{kl} . With the help of the q_{kl} , the function H_0 is

$$H_0(\lambda_p, n_p) = \ln \left[(1 - n_p) (q_{00} + q_{01} e^{i\lambda_p}) + n_p (q_{11} + q_{10} e^{-i\lambda_p}) \right]. \quad (28)$$

Using Eq. (28) we obtain for Eq. (26), with $N = \frac{e\tau}{h} V$,

$$\bar{S}_V = N \left(\phi_p \ln[q_{11} + q_{10} e^{-i\lambda_p}] + (1 - \phi_p) \ln[q_{00} + q_{01} e^{i\lambda_p}] \right). \quad (29)$$

The integral (25) is solved in saddle point approximation. The saddle point equation $\frac{\partial \bar{S}_V}{\partial \lambda_p} = 0$ is quadratic in $e^{i\lambda_p}$ and the solutions are

$$e^{i\bar{\lambda}_p(\pm)} = \frac{-q_{01}q_{10}(1 - 2\phi_p) \pm \sqrt{(q_{01}q_{10}(1 - 2\phi_p))^2 + 4q_{00}q_{01}q_{10}q_{11}\phi_p(1 - \phi_p)}}{2q_{10}q_{11}(1 - \phi_p)}. \quad (30)$$

The generating function is in saddle point approximation

$$e^{\xi(\Lambda, \phi_p)} = e^{\bar{S}_V(\Lambda, \bar{\lambda}_p, V\phi_p)}. \quad (31)$$

Only the solution $e^{i\bar{\lambda}_p(+)}$ satisfies the normalization condition $\int d\phi_p e^{\xi(\mathbf{0}, \phi_p)} = 1$.

As demonstrated in Ref. [25, 24], the saddle point approximation is correct when the delay time of the probe is much longer than the inverse average attempt frequency, $\tau_d \gg h/eV$.

To obtain the cumulants of the distribution function it is important to look at the joint generating function $S(\Lambda, m_p)$. The auto- and cross-correlations studied in section 2 can be expressed in analogy to Eqs. (19) as

$$\langle \Delta V_p^2 \rangle = V^2 \langle \Delta \phi_p^2 \rangle = -\frac{V^2 \tau}{4\pi^2} \frac{d^2 S}{dm_p^2}, \quad (32)$$

$$\langle \Delta V_p \Delta I_\alpha \rangle = \frac{V}{\tau} \langle \Delta \phi_p \Delta Q_\alpha \rangle = \frac{eV}{2\pi} \frac{d^2 S}{d\lambda_\alpha dm_p}. \quad (33)$$

The generating function $S(\Lambda, m_p)$ is in principle obtained by a Fourier transform of $\xi(\Lambda, \phi_p)$ as indicated in Eqs. (22) and (23). Another, more transparent way is to express $S(\Lambda, m_p)$ with the help of Eq. (25) and solve the coupled saddle point equations. This is shown in the appendix.

3.2. Dephasing probe.

The distribution function for the average occupation number \bar{n}_p of the dephasing probe can be found in a way similar to what is described above for the voltage probe. Here, the distribution $P_E(\mathbf{Q})$ is energy dependent and the vector \mathbf{Q} denotes the charges per energy interval, $\mathbf{Q} = \mathbf{Q}(E)dE$. The function $P_E(\mathbf{Q}, \bar{n}_p)$ is the joint probability that \mathbf{Q} charges are transmitted during τ and the average occupation number takes the value \bar{n}_p in the energy interval dE . The conjugated variable to \bar{n}_p is a number called γ_p , and the corresponding generating functions and distribution functions are $P_E(\mathbf{Q}, \bar{n}_p)$, $S_E(\Lambda, \gamma_p)$, $\xi_E(\Lambda, \bar{n}_p)$ and $\zeta_E(\mathbf{Q}, \gamma_p)$ with for example

$$P_E(\mathbf{Q}, \bar{n}_p) = \int d\Lambda \sum_{\gamma_p} e^{S_E(\Lambda, \gamma_p) + i\Lambda \mathbf{Q} + i2\pi \bar{n}_p \gamma_p}. \quad (34)$$

With this the fluctuations and correlations of section 2 are

$$\langle \Delta n_p^2 \rangle = -\frac{dE\tau}{4\pi^2} \frac{d^2 S}{d\gamma_p^2}, \quad (35)$$

$$\langle \Delta n_p \Delta i_\alpha \rangle = \frac{e}{2\pi} \frac{d^2 S}{d\lambda_\alpha d\gamma_p}. \quad (36)$$

Note that the counting fields λ_α are dimensionless and of order 1, but the variable γ_p and the generating function S scale with $dE\tau/h$, leading to the proportionality factors above. Here again, we are most interested in the distribution function

$$P_E(\bar{n}_p) = \sum_{\mathbf{Q}} P_E(\mathbf{Q}, \bar{n}_p) = e^{\xi_E(\mathbf{\Lambda}=\mathbf{0}, \bar{n}_p)}. \quad (37)$$

The function $\xi_E(\mathbf{\Lambda}, \bar{n}_p)$ is given from the stochastic path integral approach in the stationary limit:

$$e^{\xi_E(\mathbf{\Lambda}, \bar{n}_p)} = \int d\lambda_p e^{\bar{S}_E(\mathbf{\Lambda}, \lambda_p, n_p=\bar{n}_p)} = \int d\lambda_p e^{\frac{dE\tau}{h} H_0(\lambda_p, \bar{n}_p)}. \quad (38)$$

The saddle point equation $\frac{\partial H_0}{\partial \lambda_p} = 0$ is quadratic and the solution satisfying the normalization is

$$e^{i\bar{\lambda}_p} = +\sqrt{\frac{q_{10}\bar{n}_p}{q_{01}(1-\bar{n}_p)}}. \quad (39)$$

Explicitly we obtain the generating function

$$\xi_E(\mathbf{\Lambda}, \bar{n}_p) = \frac{dE\tau}{h} \ln \left[q_{00}(1-\bar{n}_p) + q_{11}\bar{n}_p + 2\sqrt{q_{10}q_{01}\bar{n}_p(1-\bar{n}_p)} \right]. \quad (40)$$

Even though the distribution function $P(\mathbf{Q})$ of the transmitted charge only is equal for both voltage and dephasing probes (in the single channel case), the generating functions Eqs. (31) and (40) are different. Technically this originates from the different structure of the saddle point equations and their solutions Eqs. (39) and (30). Physically the differences are based on the different occupation functions of the voltage and dephasing probe, a Fermi function and a non-equilibrium occupation function. As shown in Fig. 1, the later is a two-step function and carries a probabilistic uncertainty leading to different statistics of the number \bar{n}_p compared to the phase ϕ_p . This effect is already present in the fluctuations $\langle \Delta V_p^2 \rangle$ and $\langle \Delta n_p^2 \rangle$ obtained by the Langevin approach in section 2.

4. Examples.

With the formalism presented above, it is possible to discuss the full counting statistics of voltage and occupation number fluctuations and their correlations with transferred charge of the examples presented in section 2. Here we concentrate on the beam splitter, the Mach-Zehnder interferometer and the double barrier.

4.1. Beamsplitter.

The beam splitter with transmission T coupled to a probe is shown in Fig. 2. It is straightforward to evaluate the equations presented above with the expressions for q_{kl} . The q_{kl} are expansion coefficients of the determinant in Eq. (27), however for this simple example they can be found by considering the different processes in and out of the probe. q_{00} describes the process that no particle enters or leaves the probe. For the beam splitter this happens if the particle is reflected at the barrier. This process occurs with probability $1-T$. When the particle passes through the barrier with probability T , it enters the probe, this is q_{01} . The remaining q_{10} and q_{11} represent two-particle processes: no particle is injected into the probe (probability $1-T$) but one particle is

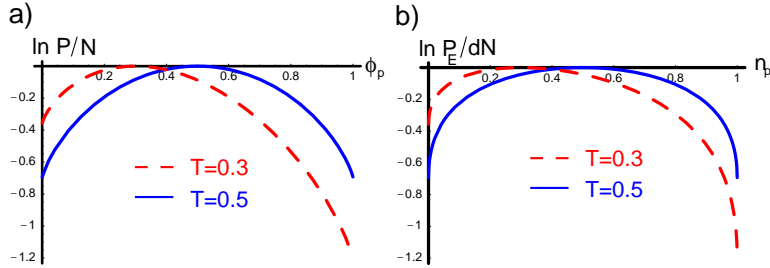


Figure 7. Distribution functions $P(\phi_p)$ of the integrated voltage (a) and $P_E(\bar{n}_p)$ of the occupation number (b) of the probe of the beam splitter for two transmission probabilities. The function $P(\phi_p)$ of the integrated voltage is a binomial distribution whereas the function $P_E(\bar{n}_p)$ of the time integrated occupation number of the dephasing probe is non-binomial. The plots are normalized with respect to $N = \frac{eV\tau}{h}$ or $dN = \frac{dE\tau}{h}$.

emitted from the probe into terminal 2 (counting factor $e^{i\lambda_2}$), or one particle enters with probability T and one leaves the probe into terminal 2. In conclusion,

$$\begin{aligned} q_{00} &= 1 - T, & q_{01} &= T, \\ q_{10} &= (1 - T)e^{i\lambda_2}, & q_{11} &= Te^{i\lambda_2}. \end{aligned} \quad (41)$$

Inserting this in Eqs.(31) and (40) we obtain

$$\xi(\lambda_2, \phi_p) = N \left(\phi_p \ln \frac{Te^{i\lambda_2}}{\phi_p} + (1 - \phi_p) \ln \frac{(1 - T)}{1 - \phi_p} \right), \quad (42)$$

$$\xi_E(\lambda_2, \bar{n}_p) = dN \ln \left[\left(\sqrt{(1 - T)(1 - \bar{n}_p)} + \sqrt{Te^{i\lambda_2}\bar{n}_p} \right)^2 \right], \quad (43)$$

with $N = \frac{eV\tau}{h}$ and $dN = \frac{dE\tau}{h}$. The two functions have a very different form. The distribution functions $P(\phi_p) = e^{\xi(0, \phi_p)}$ and $P_E(\bar{n}_p) = e^{\xi_E(0, \bar{n}_p)}$ are plotted in Fig. 7. The function $P(\phi_p)$ is a binomial distribution. Due to the saddle point approximation, the binomial factor in Eq. (42) is written approximatively. The distribution function of \bar{n}_p is non-binomial as can be clearly seen in the figure.

For this simple example the joint distribution function $P(Q, \phi_p)$ can be directly obtained with $P(Q, \phi_p) = \int \frac{d\lambda_2}{2\pi} e^{\xi(\lambda_2, \phi_p) - i\lambda_2 Q}$. We find that the distribution of the phase ϕ_p equals the distribution of the charge transmitted into a contact of the beam splitter:

$$P(Q, \phi_p) = e^{\xi(0, \phi_p)} \delta_{Q\phi_p} = P(\phi_p) \delta_{Q\phi_p}. \quad (44)$$

Also for the dephasing probe the joint distribution $P_E(Q, \bar{n}_p)$ can be calculated (in this function Q denotes the charge per energy interval). The probability function $P_E(Q, \bar{n}_p)$ depends on both variables Q and \bar{n}_p , in contrast to the voltage probe, Eq. (44) where Q and ϕ_p act effectively as one variable. This reflects the fact that the occupation number \bar{n}_p represents the probability for the emission of a particle, while the occupation in the voltage probe determines exactly each scattering event. A plot of $P_E(Q, \bar{n}_p)$ is shown in Fig. 8.

Although the two generating functions (42) and (43) have a very different form, integration over ϕ_p and \bar{n}_p respectively leads to the same generating function for charge transmitted through a beam splitter: $\ln \int_0^1 d\phi_p e^{\xi(\lambda_2, \phi_p)} = \int dE \ln \int_0^1 d\bar{n}_p e^{\xi_E(\lambda_2, \bar{n}_p)} =$

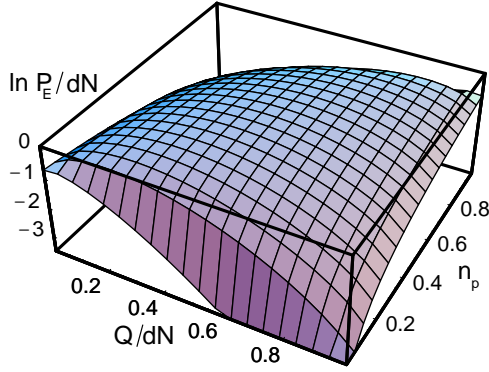


Figure 8. The joint distribution function $P_E(Q, \bar{n}_p)$ of the charge transferred into contact 2 and the integrated occupation number at the dephasing probe of the beam splitter for $T = 0.5$. In contrast to the voltage probe, the joint distribution $P(Q, \phi_p)$ is a one-dimensional binomial function with $P(Q, \phi_p) = P(\phi_p) \delta_{Q, \phi_p}$.

$N \ln[1+T(e^{i\lambda_2}-1)]$. This means that a voltage or a dephasing probe, perfectly coupled to the conductor as shown in Fig. 2 does not affect the statistics of transmitted charge.

4.2. Mach-Zehnder interferometer.

The Mach-Zehnder interferometer is shown in Fig. 3. The coefficients q_{kl} are determined by the scattering matrix and are derived in Ref. [25]:

$$q_{00} = ((R_A R_B (1 - \varepsilon) + T_A T_B) e^{i\lambda_3} + (R_A T_B (1 - \varepsilon) + T_A R_B) e^{i\lambda_4} + 2 \sqrt{R_A T_A R_B T_B (1 - \varepsilon)} \cos \Phi (e^{i\lambda_4} - e^{i\lambda_3})) \quad (45)$$

$$q_{01} = \varepsilon R_A \quad (46)$$

$$q_{10} = \varepsilon T_A e^{i(\lambda_3 + \lambda_4)} \quad (47)$$

$$q_{11} = ((R_A R_B + T_A T_B (1 - \varepsilon)) e^{i\lambda_3} + (R_A T_B + T_A R_B (1 - \varepsilon)) e^{i\lambda_4} + 2 \sqrt{R_A T_A R_B T_B (1 - \varepsilon)} \cos \Phi (e^{i\lambda_4} - e^{i\lambda_3})) \quad (48)$$

Using these parameters, the generating functions Eqs. (31) and (40) become very long expressions, which are not explicitly written out here. Plots of the functions at $\Lambda = \mathbf{0}$ are shown in Fig. 9. Note that both Eqs. (31) and (40) contain all information about the cumulants of the transmitted charge and about the phases ϕ_p and \bar{n}_p respectively. Thus both functions contain terms proportional to $\cos \Phi$ due to the interference. However the phase-dependence Φ drops out when we study cumulants of the phase ϕ_p or the occupation number \bar{n}_p of the probe. This has been already observed in section 2.3 and is explained by the setup of the MZI: particles enter the probe before they could interfere and no oscillating terms appear in the cumulants of the probe.

Interestingly, the distribution functions of ϕ_p and \bar{n}_p given by $\xi(0, \phi_p)$ and $\xi_E(0, \bar{n}_p)$ coincide to first order in the coupling parameter ε . This means that when only very few particles enter the probe, the distribution functions of the potential

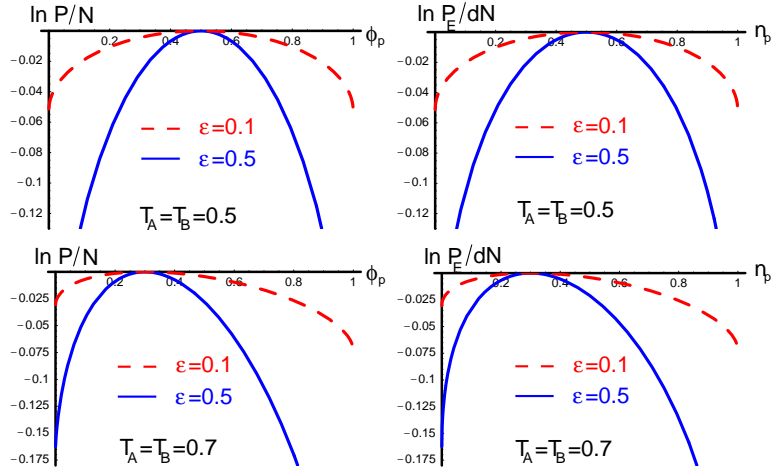


Figure 9. The distribution functions $P(\phi_p)$ (left) of the integrated voltage and $P_E(\bar{n}_p)$ (right) of the integrated occupation number of the probe of the Mach-Zehnder interferometer for different coupling strength ϵ . The case of symmetric beamsplitters is shown in the upper figures and the case of beamsplitters with transmission $T_A = T_B = 0.7$ is shown in the lower figures. For $\epsilon = 0.1$ both distribution functions look very similar (in fact they are equal to first order in ϵ). For stronger coupling, the tails of the distribution are broader for the dephasing probe. The maximum of both distribution functions lies at $R_A = 1 - T_A$.

and of the occupation function per energy respectively behave similarly, while for a higher number of charges in the probe the differences become more and more clear, in particular the function $P(\phi_p)$ is narrower than $P_E(\bar{n}_p)$.

4.3. Double barrier.

The double barrier is shown in Fig. 4. In this setup the electrons enter the probe after they interfere and the distribution function depends on the phase picked up. The coefficients q_{kl} are

$$q_{00} = \frac{R_1 + (1 - \epsilon)(R_2 + T_1 T_2 e^{i\lambda_2}) + 2\sqrt{R_1 R_2 (1 - \epsilon)} \cos \Phi_d}{1 + R_1 R_2 (1 - \epsilon) + 2\sqrt{R_1 R_2 (1 - \epsilon)} \cos \Phi_d} \quad (49)$$

$$q_{01} = \frac{R_1 T_2 e^{i\lambda_2} \epsilon}{1 + R_1 R_2 (1 - \epsilon) + 2\sqrt{R_1 R_2 (1 - \epsilon)} \cos \Phi_d} \quad (50)$$

$$q_{10} = \frac{T_1 \epsilon}{1 + R_1 R_2 (1 - \epsilon) + 2\sqrt{R_1 R_2 (1 - \epsilon)} \cos \Phi_d} \quad (51)$$

$$q_{11} = \frac{R_1 (1 - \epsilon) + R_2 + T_1 T_2 e^{i\lambda_2} + 2\sqrt{R_1 R_2 (1 - \epsilon)} \cos \Phi_d}{1 + R_1 R_2 (1 - \epsilon) + 2\sqrt{R_1 R_2 (1 - \epsilon)} \cos \Phi_d} \quad (52)$$

Plots of the distribution functions of the voltage probe and the dephasing probe, Eqs. (31) and (38) at $\lambda_2 = 0$ are shown in Fig. 10. Both functions depend on the phase and are most narrow at $\Phi_d = \pi$. Around this value the differences between the voltage and dephasing probe become visible: the distribution function $P(\phi_p)$ is narrower than $P_E(\bar{n}_p)$. For values further away from π the functions look pretty much

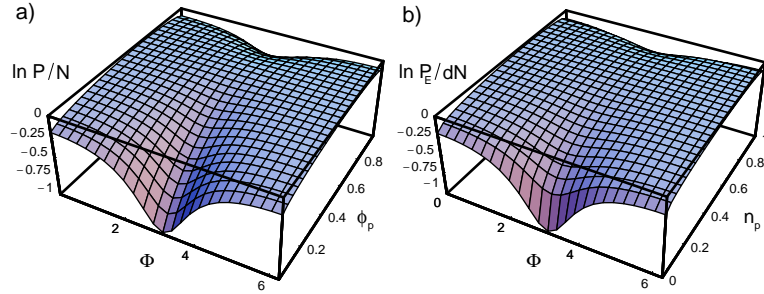


Figure 10. The distribution function $P(\phi_p)$ for the integrated voltage (a) and $P_E(\bar{n}_p)$ for the integrated occupation number (b) of the probe of the double barrier geometry for equal transmission probabilities $T_1 = T_2 = 1/2$ and $\varepsilon = 1 - e^{-1}$ as a function of the phase Φ_d . The different properties of the two probes are most apparent around $\Phi_d = \pi$.

alike. Since the transmission T_{p1} has a maximum in $\Phi_d = \pi$, this is in agreement with our findings that the more particles enter the probe the less broad are the distribution functions.

5. Conclusions.

In this work, using the Langevin approach, we examined the auto-correlations of voltage fluctuations at voltage probes and occupation number fluctuations at dephasing probes. We investigated correlations between voltage (or occupation number) fluctuations at probes and currents at a contact of the conductor. We determined these fluctuation spectra for several examples. Subsequently we extended this discussion to include higher order cumulants. To achieve this we extended a stochastic path integral approach to find the generation function for the distribution of voltage and occupation number fluctuations and also the joint distribution of voltage (or occupation number) fluctuations and current fluctuations. Interestingly we find differences between the fluctuations of voltage and dephasing probes despite the fact that for single channel probes the full counting statistics of the transmitted currents is identical [24, 25]. This is a consequence of the fact that occupation numbers at different energies in the dephasing probe are uncorrelated while in a voltage probe they are correlated. The fluctuations of the occupation number of a dephasing probe are larger than the potential fluctuations of a voltage probe. For small coupling of the probe -corresponding to a small number of particles entering the probe- the differences become less important. It is expected that dephasing and which path detection are closely related. To understand this we analyzed the sensitivity of the correlation functions of voltage (or occupation number fluctuations) and currents to Aharonov-Bohm oscillations. For the examples investigated here, we found that the Aharonov-Bohm effect in the loop directly probed by the voltage or dephasing contact is indeed absent. However, further research is needed to determine whether this is general for voltage and dephasing probes or whether this is simply a property of the examples investigated here.

Acknowledgment.

This work was supported by the Swiss NSF, the Swiss National Center of Competence in Research MaNEP, the European Marie Curie MCTR-CT-2003-504574 and the Swedish VR.

Appendix A. Stochastic path integral.

We show how the Eq. (25) for the voltage probe is obtained starting from the stochastic path integral approach [4, 12]. The voltage probe is described by a Fermi function with a potential $V_p(t)$ fluctuating on the time scale τ_d . As derived in detail in Ref. [25], the generating function $S_V(\Lambda)$ (the index V stands for voltage probe) is given by the stochastic path integral

$$e^{S_V(\Lambda)} = \int \mathcal{D}V_p \mathcal{D}\lambda_p e^{\tilde{S}_V(\Lambda, \lambda_p, V_p)} \quad (\text{A.1})$$

$$\tilde{S}_V = \frac{1}{h} \int_0^\tau dt \left[-i\tau_d \lambda_p e \dot{V}_p + \int dE H_0 \right]. \quad (\text{A.2})$$

The function H_0 is defined by Eq. (27) and is determined by the scattering matrix. The term $-i\tau_d \lambda_p e \dot{V}_p$ results from the charge conservation on the probe. The path integral in V_p and λ_p is evaluated via a saddle point approximation which is a good approximation for $\tau_d \gg h/eV$. For a discussion of this important point see Refs. [24, 25]. For a long measurement time $\tau \gg \tau_d$, the function \tilde{S}_V is stationary in the variables λ_p and V_p , and the saddle point equations are:

$$\frac{\partial \tilde{S}_V}{\partial \lambda_p} = 0, \quad \frac{\partial \tilde{S}_V}{\partial V_p} = 0 \quad \text{with } \tilde{S}_V = \frac{\tau}{h} \int dE H_0. \quad (\text{A.3})$$

Starting from Eq. (A.1) we also find the full counting statistics of the probe.

We define a joint probability $P(\mathbf{Q}, \phi_p)$ that \mathbf{Q} charges are transmitted and the phase due to the potential at the probe is ϕ_p . With Eq. (A.1) the joint probability $P(\mathbf{Q}, \phi_p)$ is given by

$$P(\mathbf{Q}, \phi_p) = \int \mathcal{D}V_p \delta \left(\phi_p - \frac{1}{V\tau} \int_0^\tau dt V_p(t) \right) \int d\Lambda \mathcal{D}\lambda_p e^{\tilde{S}_V(\Lambda, \lambda_p, V_p) - i\Lambda \mathbf{Q}}. \quad (\text{A.4})$$

Here the constraint $\phi_p = 1/(V\tau) \int dt V_p(t)$ is introduced via a functional delta function $\delta(\phi_p - \frac{1}{V\tau} \int_0^\tau dt V_p(t)) = \sum_{m_p} \exp(2\pi i m_p (\phi_p - \frac{1}{V\tau} \int_0^\tau dt V_p(t)))$. Inserting the sum we find

$$P(\mathbf{Q}, \phi_p) = \int d\Lambda \sum_{m_p} e^{S(\Lambda, m_p) - i\Lambda \mathbf{Q} + 2\pi i \phi_p m_p} \quad (\text{A.5})$$

where the generating function is given by

$$e^{S(\Lambda, m_p)} = \int \mathcal{D}V_p \mathcal{D}\lambda_p e^{\tilde{S}_V(\Lambda, \lambda_p, V_p) - \frac{2\pi i m_p}{V\tau} \int_0^\tau dt V_p(t)}. \quad (\text{A.6})$$

In the stationary limit the path integrals in λ_p and V_p are reduced to ordinary integrals. Then the sum in m_p in Eq. (A.5) can be evaluated giving a delta function $\delta(\phi_p - V_p/V)$ and thus

$$P(\mathbf{Q}, \phi_p) = \int d\Lambda \int d\lambda_p e^{\tilde{S}_V(\Lambda, \lambda_p, V_p = V\phi_p) - i\Lambda \mathbf{Q}} = \int d\Lambda e^{\xi(\Lambda, \phi_p) - i\Lambda \mathbf{Q}} \quad (\text{A.7})$$

leading to Eq. (25).

In order to obtain the joint generating function $e^{S(\Lambda, m_p)}$ directly, it is convenient to start from Eq. (A.6). In the stationary case, we have to solve the coupled saddle point equations in ϕ_p and λ_p . Up to a constant, the solution is

$$S(\Lambda, m_p) = N \ln \left[q_{00} + q_{11} e^{-\frac{2\pi i m_p}{N}} + \sqrt{\left(q_{00} - q_{11} e^{-\frac{2\pi i m_p}{N}} \right)^2 + 4 q_{01} q_{10} e^{-\frac{2\pi i m_p}{N}}} \right] \quad (\text{A.8})$$

The cumulants like the auto- and cross-correlations shown in Eqs. (32) and (33) are then given by simple derivations of the above function $e^{S(\Lambda, m_p)}$ taken at $\Lambda = m_p = 0$.

For the dephasing probe, the procedure outlined here is exactly the same, but all functions concern an energy interval of width dE . However, the joint generating function $S_E(\Lambda, \gamma_p)$ can not be obtained exactly unlike for the voltage probe.

References

- [1] Ya. M. Blanter and M. Büttiker, Phys. Rep. **336**, 1 (2000).
- [2] L. S. Levitov, H. Lee, and G. B. Lesovik, J. Math. Phys. **37**, 4845 (1996).
- [3] *Quantum Noise in Mesoscopic Physics*, edited by Yu. V. Nazarov (Kluwer, Dordrecht, 2003).
- [4] S. Pilgram, A. N. Jordan, E. V. Sukhorukov, and M. Büttiker, Phys. Rev. Lett. **90**, 206801 (2003).
- [5] K. E. Nagaev, Phys. Rev. B **66**, 075334 (2002).
- [6] B. Reulet, J. Senzier, and D. E. Prober, Phys. Rev. Lett. **91**, 196601 (2003).
- [7] Yu. Bomze, et al., Phys. Rev. Lett. **95**, 176601 (2005).
- [8] S. Gustavsson, et al., Phys. Rev. B **74**, 195305 (2006).
- [9] T. Fujisawa, T. Hayashi, R. Tomita, Y. Hirayama, Science **312**, 1634 (2006).
- [10] A. V. Timofeev et al., cond-mat/0612087.
- [11] S. Pilgram and M. Büttiker, Phys. Rev. B **67**, 235308 (2003).
- [12] A. N. Jordan, E. V. Sukhorukov and S. Pilgram, J. Math. Phys. **45**, 4386 (2004).
- [13] G. Seelig, S. Pilgram, A. N. Jordan, and M. Büttiker, Phys. Rev. B **68**, 161310 (2003).
- [14] M. Kindermann, Yu. V. Nazarov, C. W. J. Beenakker, Phys. Rev. Lett. **90**, 246805 (2003).
- [15] P. J. Hakonen, A. Paila, and E. B. Sonin, Phys. Rev. B **74**, 195322 (2006).
- [16] M. Kindermann, Yu. V. Nazarov, and C. W. J. Beenakker, Phys. Rev. B **69**, 035336 (2004).
- [17] M. Büttiker, IBM J. Res. Develop., **32**, 63-75 (1988).
- [18] C. W. J. Beenakker and M. Büttiker, Phys. Rev. B **46**, 1889 (1992).
- [19] C. Texier and M. Büttiker, Phys. Rev. B **62**, 7454 (2000).
- [20] S. Oberholzer, et al., Phys. Rev. Lett. **96**, 046804 (2006).
- [21] M. J. M. de Jong and C. W. J. Beenakker, Physica A **230**, 219 (1996).
- [22] M. Büttiker, Phys. Rev. Lett. **65**, 2901 (1990).
- [23] M. Büttiker, Phys. Rev. B **46**, 12485 (1992).
- [24] S. Pilgram, P. Samuelsson, H. Förster, and M. Büttiker, Phys. Rev. Lett. **97**, 066801 (2006).
- [25] H. Förster, P. Samuelsson, S. Pilgram, and M. Büttiker, cond-mat/0609544.
- [26] A. Stern, Y. Aharonov, Y. Imry, Phys. Rev. A **41**, 3436 (1990).
- [27] P. W. Brouwer and C. W. J. Beenakker, Phys. Rev. B **55**, 4695 (1997).
- [28] M. Büttiker, in *Quantum Noise in Mesoscopic Physics*, edited by Yu. Nazarov (Kluwer, Dordrecht, 2003). p.3
- [29] A. A. Clerk and A. D. Stone, Phys. Rev. B **69**, 245303 (2004).
- [30] S.-W. V. Chung, M. Moskalets, P. Samuelsson, cond-mat/0611580.
- [31] S. A. van Langen and M. Büttiker, Phys. Rev. B **56**, R1680 (1997).
- [32] S. Oberholzer, et al., Physica E **6**, 314 (2000).
- [33] W. D. Oliver, J. Kim, R. C. Liu, and Y. Yamamoto, Science **284**, 299 (1999).
- [34] G. Seelig and M. Büttiker, Phys. Rev. B **64**, 245313 (2001).
- [35] F. Marquardt and C. Bruder, Phys. Rev. Lett. **92**, 56805 (2004).
- [36] F. Marquardt and C. Bruder, Phys. Rev. B **70**, 125305 (2004).
- [37] H. Förster, S. Pilgram, and M. Büttiker, Phys. Rev. B **72**, 075301 (2005).
- [38] V. S.-W. Chung, P. Samuelsson, and M. Büttiker, Phys. Rev. B **72**, 125320 (2005).
- [39] Y. Ji, et al., Nature **422**, 415 (2003).
- [40] L. V. Litvin, H.-P. Tranitz, W. Wegscheider, and C. Strunk, cond-mat/0607758.
- [41] I. Neder, et al., Phys. Rev. Lett. **96**, 016804 (2006).
- [42] E. V. Sukhorukov and V. V. Cheianov, cond-mat/0609288.

- [43] I. Neder, et al., cond-mat/0610634.
- [44] I. Neder and F. Marquardt, cond-mat/0611372.
- [45] B. J. Van Wees, et al., Phys. Rev. Lett. **62**, 2523 (1989).
- [46] B. W. Alphenaar, et al., Phys. Rev. B **46**, 7236 (1992).
- [47] N. C. van der Vaart, et al., Phys. Rev. Lett. **74**, 4702 (1995).
- [48] G. Kießlich, P. Samuelsson, A. Wacker, and E. Schöll, Phys. Rev. B **73**, 033312 (2006).
- [49] S. Jakobs, V. Meden, H. Schoeller, and T. Enss, cond-mat/0606486.
- [50] L. S. Levitov and G. Lesovik, JETP Lett. **58**, 230 (1993).
- [51] P. San-Jose and E. Prada, Phys. Rev. B **74**, 045305 (2006).